Optimization of WEDM process parameters for machining hybrid composites (LM6/B₄C/Fly Ash)

Jayavelu Udaya Prakash[1], Charles Sarala Rubi[2],
Sunder Jebarose Juliyana[1], Sachin Salunkhe[3,4]*, H. B. Özerkan[4]
and Lenka Cepova[5]

[1]Department of Mechanical Engineering, Vel Tech Rangarajan Dr. Sagunthala R&D Institute of Science and Technology, Chennai, India, [2]Department of Physics, Vel Tech Rangarajan Dr. Sagunthala R&D Institute of Science and Technology, Chennai, India, [3]Department of Biosciences, Saveetha School of Engineering, Saveetha Institute of Medical and Technical Sciences, Chennai, India, [4]Department of Mechanical Engineering, Faculty of Engineering, Gazi University, Ankara, Türkiye, [5]Department of Machining, Assembly and Engineering Metrology, Faculty of Mechanical Engineering, VSB-Technical University of Ostrava, Ostrava, Czechia

Introduction: Wire-electric discharge machining (WEDM) possesses multiple benefits over traditional production approaches; it allows for the precise processing of complex and rigid particulate-reinforced composite materials. Aluminium alloys have found widespread applications in surgical components, shipbuilding, aircraft, automobiles, and inhaling gas cylinders for scuba diving, due to its good strength, and light weight properties.

Methods: The main aim of this investigation is to optimize different process variables for LM6/B₄C/Fly ash particle reinforced hybrid composites using WEDM to attain performance metrics such as maximum material removal rate (MRR) and minimal surface roughness (SR). Taguchi's L_{27} orthogonal array (OA) matrix and Grey Relational Analysis (GRA) were used.

Results and Discussion: According to ANOVA, the two variables with the most significant impact on MRR and SR are gap voltage and reinforcement percentage, with respective impacts of 29.59% and 20.69%. When the composite is machined, the following process variables work best: GV of 30 V, T_{on} of 10 μs, T_{off} of 2 μs, WF of 4 m/min, and R of 6%. A low gap voltage causes the erosion to rise and the MRR to increase. However, SR will also increase which is undesirable, so optimum gap voltage values are required for WEDM.

KEYWORDS

hybrid composites, stir casting, Taguchi's DOE, WEDM, ceramic particles

1 Introduction

Composites are composed of two different phases; the principal constituent is the continuous phase (matrix) and involved, which is the dispersion of the discrete component (reinforcement particles). The geometrical shapes and forms of the two phases differ, and the interface features determine the composite's characteristics. Mechanical characteristics like hardness, rigidity, and abrasiveness, among others, are imparted by the reinforcement particles. The continuous phase and reinforcement particles have intrinsically superior characteristics to any parent elements (Juliyana et al., 2022a). The most widely employed MMC in the industry is aluminum matrix composites or AMCs. Aluminum is widely

employed in today's market because of its many advantageous features, which include excellent strength, low weight, and good resistance to corrosion. Generally, abrasive ceramic particles such as SiC, Al_2O_3, ZrO_2, and others strengthen aluminum alloys of various proportions and grades (Prakash et al., 2023a). MMC design aims to combine the best qualities of metal and ceramic particles. When ductile metal is mixed with refractory particles, a material with mechanical characteristics is created halfway between the matrix and ceramics (Jayaseelan et al., 2023). Metals have unique qualities, including robustness, ductility, and tolerance to high temperatures but also low stiffness. Conversely, ceramic particles are robust and stiff yet easily broken (Prakash et al., 2018). Because of their poor surface finish and high tool degradation rate, particle-reinforced hybrid MMCs are typically highly difficult and challenging to machine using traditional machining techniques (Laghari et al., 2023). Since WEDM is comparatively devoid of the challenges typically encountered when machining using conventional machining techniques, it may be a viable substitute for the professional machining of such substances (Fanani et al., 2021). Using a dielectric foil between the specimen and the tool and a pulsing direct-current power source, the WEDM technique rapidly and repeatedly discharges sparks to remove the material (Bains et al., 2016). Each discharge melts or evaporates a tiny portion of the specimen's surface. After cooling in the dielectric fluid, the melted metal solidifies into tiny spherical fragments. However, the narrower kerf and higher spark frequency cause the particles to remain in the machining zone rather than being evacuated (Qudeiri et al., 2020). On the outer surface of the specimen, the remaining components usually solidify again and form a very brittle layer known as the recast layer (Sarala Rubi et al., 2024). Furthermore, it has also been documented that creating a heat-affected zone results in microcracks, which typically cause the machined components to become damaged early in their functional lifespan (Lee and Tai, 2003). Depending on the parameter used for cutting, the recast layer seen during the machining of a thermally inefficient material such as pure titanium thickness ranges from 6 to 58 μm (Kumar et al., 2013). Peak current and T_{on} have been found to increase the recast layer generally (Omole et al., 2022). WEDM is excellent for creating complicated or elaborate structures that are challenging to manufacture with a regular technique. WEDM is widely used in several areas, such as tool and die manufacturing companies, space applications, and the automotive industry (Goyal et al., 2022). All conductive materials have been machined using this method for the past 10 years. As time has passed, electrically conductive materials can now be cut without concern about their range owing to the Electrical Discharge Machining technique (Prakash et al., 2021). Techniques like ANN, fuzzy logic, and evolutionary algorithms have drawn more interest to WEDM from researchers in the past 10 years (Juliyana et al., 2022b). In addition to sophisticated algorithms, fundamental component analysis and Taguchi optimization methodologies have become popular mathematical approaches (Prakash et al., 2023b). There are numerous methods to define the goal function in the EDM and WEDM procedures in order to provide remedies to multi-response optimization challenges (Ananth et al., 2021; Srinivasa Rao et al., 2016). Brass, tungsten, and copper wires with a width of 0.005–0.3 mm are the wires that are used in WEDM, and the deionized water acts as a dielectric medium. When a wire comes into contact with a de-ionized water molecule,

it produces more electrons. This process proceeds in the direction of the anode since the electrons' kinetic energy is converted into heat energy, which produces a spark. Electric discharges caused by this action cause the material to melt and vaporize, and dielectric fluid drives the particles out and away from them. This is continuously maintained by a positioning system controlled by a computer.

Thus, the most important objectives are to maximize MRR and minimize SR (Calvo and Daniel, 2019; Rubi et al., 2022). Using Taguchi's L_{16} OA, GRA, and ANOVA, Durairaj et al. (2013) examined SS304 to optimize the factors such as GV, WF, T_{on}, and T_{off}, along with specific fixed parameters for achieving the lowest k_w and SR in WEDM. Similarly, a study by Lodhi and Agarwal (2014) used wire feed and criteria, including T_{on}, T_{off}, and IP, to examine the SR of AlSl D3 steel in WEDM. Taguchi's L_9 OA and ANOVA were employed to maximize the outcomes. It is discovered that the discharge current influences SR most significantly. Furthermore, Singh and Pradhan (2014) and Manjaiah et al. (2016) used Taguchi's OA technique and ANOVA in combination with RSM to examine the machining variables. The T_{on} and servo voltage are the most significant variables for the findings.

Additionally, Goswami and Kumar (2014) examined the Nimonic 80-A alloy by considering WEDM input variables and using a multi-response optimization approach to investigate how this affected the machined surface's features. Additionally, Kumar et al. (2018) used RSM, GRA, and ANOVA to optimize the MRR, SR, and kerf width responses by examining the WEDM parameters on HSS M2 grade. However, Marelli et al. (2019) used Taguchi's OA, GRA, ANN, and PCA to examine the multiple input variables involved in WEDM on superalloys to improve responses like MRR and SR. Titanium alloys have been the subject of numerous investigations. Using Taguchi's L_{18} OA, Nourbakhsh et al. (Nourbakhsh et al., 2013) analyzed the impacts of several WEDM input variables to ascertain the machining efficiency. Likewise, Silambarasan and Prabhakaran (2019) selected L_{18} OA and Genetic Algorithm (GA) techniques for optimum SR and MRR by analyzing the different WEDM input variables for titanium grade 5 alloys. Furthermore, Magabe et al. (2019) used L_{16} DoE, ANOVA, and GA methods to analyze the effectiveness of WEDM process parameters on $Ni_{55.8}Ti$ alloy for the outputs MRR and SR. In addition, using Taguchi DoE and ANOVA, Pramanik et al. (2019) analyzed the errors produced in the shape of holes by incorporating process parameters like WT and T_{on} in WEDM for Ti_6Al_4V alloy. In contrast, Thangaraj et al. (2020) used the Taguchi–GRA-based strategy to examine the surface features of the micro-titanium alloy. Paulson et al. (2023) used Taguchi's L_{18} OA to assess the various WEDM parameters for titanium superalloy to achieve the best SR and MRR. The findings demonstrate that T_{off} and IP impact how well the process performs. The complex and demanding process of micro WEDM and its impact on the aluminum was analyzed by Somashekhar et al. (2012). Study conducted by Ramanan on Al7075 alloy using active charcoal as second phase material using Grey - Fuzzy approach. The goal was to increase the MRR while minimizing the SR and overcut. For WEDM, samples with significant weight levels, hardness impact resistance, and final breaking strength are chosen for evaluation. Fuzzy GRA is utilized to increase MRR and decrease SR for the optimal machining variables based on the outcome of these variables (Ramanan and Edwin Raja Dhas, 2017). Singh and Misra (2018) used RSM to determine the impact of

TABLE 1 Chemical composition of aluminum alloy (LM6).

Constituent	Si	Cu	Fe	Mg	Mn	Ti	Ni	Zn	Al
Weight %	11.48	0.013	0.52	0.02	0.01	0.02	0.01	0.01	Remainder

several machining variables, including T_{on}, T_{off}, IP, and SV, on the machining of Nimonic C263 superalloy. According to the authors, the most significant machining variable affecting the CS was T_{on}, which IP followed. It became apparent that the servo voltage and T_{off} were less efficient. It was also discovered that the process variables impacted the CS. A study using brass wire cryogenically processed during the machining of Nimonic 80A revealed that a rise in IP causes the MRR to increase and the SR to decrease. However, the FR significantly impacted neither the MRR nor the SR (Goyal et al., 2017). In order to arrive at the best responses with the least amount of tool wear, Vishwakarma et al. (2012) examined a variety of advanced modern materials, including nanoparticles, ceramic particles, super alloys, and MMCs, on a variety of unconventional machining processes. Karthik et al. (2019) used Taguchi's L_{18} OA to optimize the WEDM variables to achieve improved surface finish, MRR, and decreased K_w. In addition, Kumar et al. (2022) used EDS and SEM analysis to investigate the machining parameters in WEDM for aluminum hybrid composites to optimize results like MRR, SR, and spark gap.

It is clear from the literature that the WEDM has been used for making complex shapes with various materials. Thus, to achieve affordable and high-quality machining, the optimum process parameters must be used. Finding the optimized machining settings for WEDM of fabricated hybrid composite plates (LM6/B$_4$C/Fly Ash) is the main aim of this research work. Grey relational analysis has been utilized to identify the optimum process parameters.

2 Materials and methods

The materials used in this investigation were selected based on cost, use, and quality. Stir casting is a liquid-state fabrication method that combines particle reinforcement with a melted LM6 alloy (Parikh et al., 2021). Three plates measuring 100 mm by 100 mm by 10 mm with reinforcement weight percentages of 3, 6, and 9 were fabricated accordingly.

2.1 Materials

2.1.1 LM6 alloy

Aluminum alloys, such as LM6 alloy, are challenging to process because of their propensity to drag and high Si content, which accelerates tool wear. The LM6 alloy has remarkable resistance to corrosion in both typical marine and atmospheric environments. Table 1 displays the chemical composition of the aluminum alloy.

2.1.2 Boron carbide (B$_4$C)

For this investigation, 63-micron-sized B$_4$C particles were employed as one type of reinforcement material. B$_4$C is widely
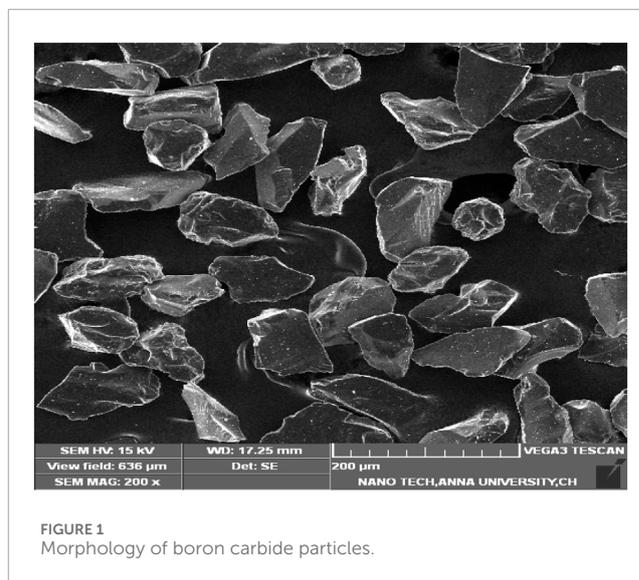
FIGURE 1
Morphology of boron carbide particles.

employed as cermets and armor materials due to its many desirable qualities (Udaya Prakash et al., 2021). Components containing materials with a high neutron absorption cross-section in a nuclear reactor are used as control rods. Therefore, boron carbide is very well suited. Figure 1 depicts the morphology of the B$_4$C particles.

2.1.3 Fly ash

Fly ash is another reinforcement material with a particle size of 12-micron. CaO, SiO$_2$, Al$_2$O$_3$, and Fe$_2$O$_3$ are the main components of fly ash. The resistance to wear, damping qualities, hardness, stiffness, and density of LM6 alloys are all improved by including fly ash. Given their low cost and low density, fine-grained fly ash particles—a waste byproduct of thermal power plants—can be discrete fragments utilized in metal matrix composites (Sadhana et al., 2020). Fly ash is readily available in large quantities. Figure 2 depicts the morphology of fly ash particles.

2.2 Fabrication of hybrid composite materials

The LM6 alloy ingots were placed in a graphite crucible and gradually heated to 850°C. The melt had been degassed at 800°C using hexa chloro ethane. Fly ash and B$_4$C particles heated to 250°C were added to the molten metal after it had been agitated to form a vortex. The slurry was agitated at 600 rpm for 10 min. In order to increase the wettability and interfacial bonding, Potassium hexa fluoro titanate (K$_2$TiF$_6$, 1% wt) was added to the Al/B$_4$C composite casting process to generate a reaction layer on an interface. Mg
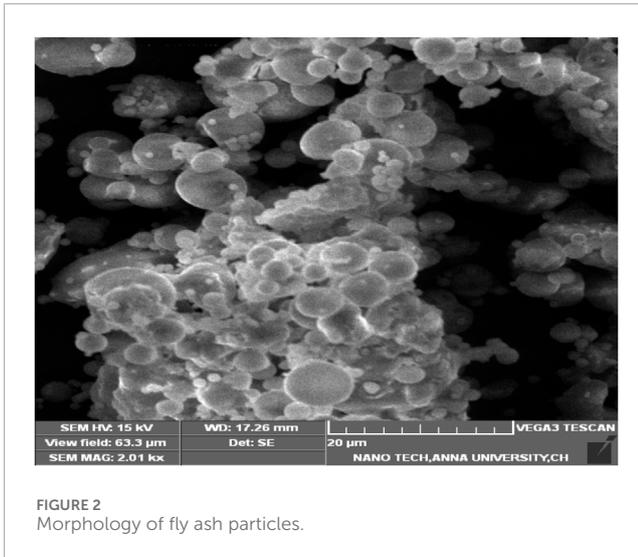
FIGURE 2
Morphology of fly ash particles.

FIGURE 3
Stir casting setup with furnace.

was added to enhance the ability to wet fly ash particles (Rubi and Prakash, 2020). After being agitated and distributed, the molten metal was poured into a 650°C preheated mold and cooled. Three hybrid composites at weight percentages of 3, 6 and 9% were produced by adding boron carbide (1.5, 3, and 4.5 wt%) and fly ash (1.5, 3, and 4.5 wt%) with LM6 Al alloy. Figure 3 displays the stir-casting equipment utilized during the manufacturing technique.

2.3 Design of experiments

The Design of Experiments (DoE) technique is used to specify what information, in what amount, and under what conditions needs to be gathered during an experiment to meet two primary objectives: lower costs and improved statistical accuracy of the response parameters (JebaroseJuliyana et al., 2023a). Five distinct process parameters were chosen for the current investigation: wire feed (WF), reinforcement percentage (R), gap voltage (GV),

pulse on time (T_{on}), and pulse off time (T_{off}). The responses are SR and MRR. The L_{27} array is chosen for this inquiry based on the chosen parameters. The unique feature of the L_{27} array is that it partially confounds two-way interactions between several factors with different columns, which reduce their impact on estimating the main effects of the different parameters. There are three levels for each of the five parameters. As a result, the complete factorial design must be used in $3^5 = 243$ experiments; however, DoE was only used in 27 experiments. Thus, 216 trials were trimmed down. 1 out of 9 experiments were carried out, saving 88% of the time and materials. For every experimental condition, three repetitions of the experiment have been conducted. Table 2 shows the machining variables together with their respective levels.

2.4 WEDM of hybrid composites

WEDM is an innovative machining technique that efficiently uses electricity to cut any material that transmits electricity. In the WEDM process, the work piece carries the positive electrical charge, while the wire carries the negative. As the wire approaches the element, the magnetism of electrical charges causes a controlled spark to form, melting and utilizing it to vaporize tiny particles. The spark removes a tiny amount of the wire because it only goes through the specimen once (JebaroseJuliyana et al., 2023b).

The method generates thousands of sparks every second, but the wire never contacts the specimen. A dielectric solution called de-ionized water cleanses and cools the cutting area. The fluid also functions as an electrically inert shield in the machining region to prevent the development of electrically conducting channels. An electrical spark results from a current passing between the wire and the specimen when the wire approaches the material, and the force of the electric field overcomes the barrier (Juliyana et al., 2022c). Machined composites are shown in Figure 4.

2.5 Grey relational analysis (GRA)

Using GRA, machining variables can be optimized multi-objectively. Discrete data, various inputs, and enhanced uncertainty management are all offered by the Grey Relational Theory. Grey may be used to forecast the approximate sequence correlation and provide a good assessment of the exact degree of data variance among sequences (Peter et al., 2014). The following procedures could be taken in order to optimize process variables:

i.   Normalizing the responses of the investigation.
ii. Figure out the variance's order.
iii. Computing the grey relational coefficient (GRC).
iv. Determining the Grey relational grade (GRG).
v.   Using ANOVA and GRG, the experimental data was analyzed.
vi. Determining the optimum process variables.
vii. Conducting confirmation experiments to verify the optimal variables.

TABLE 2 Machining input parameters and their levels.

Level	Machining parameters				
	Gap voltage (V)	Pulse on time (µs)	Pulse off time (µs)	Wire feed (m/min)	Reinforcement %
1	30	2	2	4	3
2	50	6	6	6	6
3	70	10	10	8	9
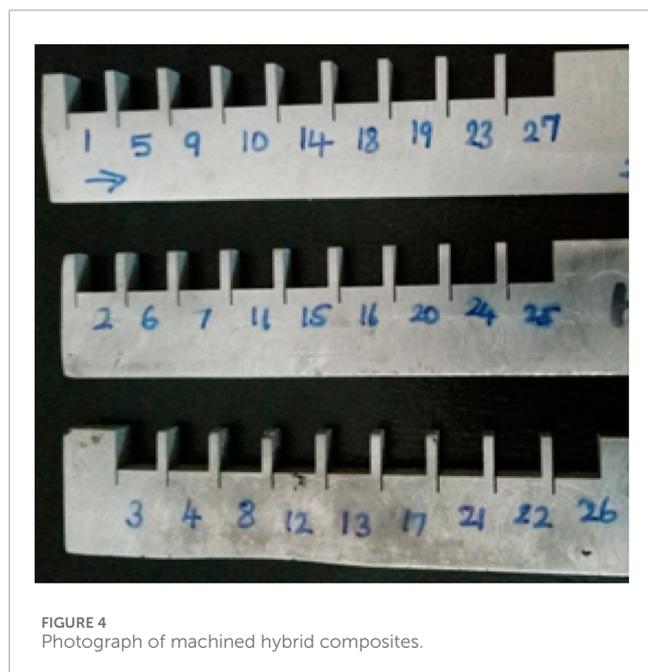
FIGURE 4
Photograph of machined hybrid composites.

3 Results and discussion

3.1 Microstructural analysis

The main objective of microstructural analysis is to confirm the uniform distribution of reinforcement particles in the matrix. An optical microscope was utilized to analyze the composite materials' microstructure. The optical photomicrographs show the homogeneous distribution of reinforcement particles within the continuous phase—Figure 5 displays micrographs of LM6 alloy and hybrid composites. The Al-Si eutectic particles in these alloys resemble spikes and scripts, respectively. However, LM6 alloys have higher silicon content; more Al-Si particles are in them. The Al-Si in LM6 (Figure 5A) has a more extended acicular arm.

The dispersion of the 3% hybrid (fly ash and B_4C particles) in the aluminum matrix composites is depicted in Figure 5B. The photomicrographs of the LM6 alloy's hybrid MMC with a 6% inclusion of hybrid particulate materials are displayed in Figure 5C. Al-Si is finer, and the dispersion of composites is even. The microstructure of the 9% hybrid AMCs is shown in Figure 5D. The pattern of dispersion is uniform in LM6 alloys. The greater

silicon content in LM6 alloys preserves this unique, evenly distributed pattern.

3.2 Experimental results

Multi-objective optimization was used to simultaneously achieve the highest MRR and smallest SR values. The 27 rows of the L_{27} orthogonal array, which corresponds to the number of trials with 13 columns and three levels, were selected. Table 3 lists the input process parameters, investigation's outcomes such as MRR, SR, Grey Relational Grades and their ranks.

3.3 Analysis and discussion

Plots were created to show the main effects of the process factors on the GRG data. Response graphs, sometimes called the main effects plot, are used to analyze the parametric effects on the response features. The GRG data undergoes ANOVA to ascertain the significance of each variable and its effect on the response features.

The optimum values of the machining parameter are determined by examining the response graphs and the response table. Figure 6 shows that the GRG rises with the rise of T_{on} and decrease of GV, T_{off}, wire feed, and reinforcement. A larger MRR results from more discharges occurring in a particular period when the T_{off} drops. The standard discharge gap widens as gap voltage rises, producing minimal SR values. Reinforcement of hard particles decreases the MRR. The wire feed is not significant.

3.4 Selection of optimal levels

Table 4 displays the mean value of each response feature for each variable level. The order of significance shows how important each factor is in the response. According to the ranks and delta values, GV, reinforcement, T_{off}, WF, and T_{on} are the variables that have the most impact on achieving maximum GRG. Figure 6 illustrates how the first level of wire feed, the second level of reinforcement, the third level of T_{on}, the first level of T_{off}, and the first level of GV produce the optimal values. The significance of the process parameters in connection to GRG was investigated using ANOVA. The F-values from the table are $F_{0.05, 2,12} = 3.89$ and $F_{0.05,4,12} = 3.26$ at the 5% significance level. ANOVA Table 5 suggests that the GV and percentage reinforcement were significant.
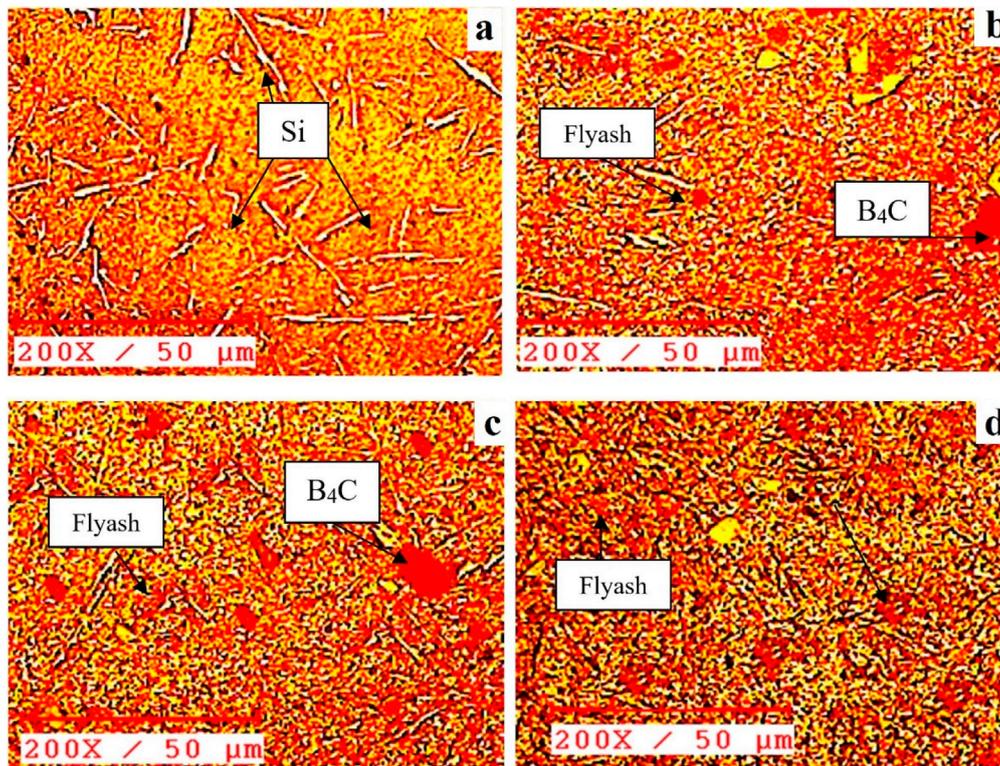
FIGURE 5
(A–D) Micrographs of B_4C/Fly Ash reinforced hybrid AMCs.

3.5 Confirmation experiments

Analyzing the experimental data determines the most effective responses. The variables at levels A_1, B_3, C_1, D_1, and E_2, which are GV 30 V, T_{on} 10 μs, T_{off} 2 μs, WF 4 m/min, and R 6%, are the optimum values for attaining the largest MRR and minimal SR. The experimental value of GRG is 0.733, while the predicted value is 0.711.

3.6 The effect of WEDM process variables on the GRG

3.6.1 Effect of gap voltage on GRG

A low voltage causes the erosion to rise and the machining rate to increase. However, undesirable SR will also result in increased MRR. As a result, relatively modest voltage values are required for WEDM. The findings indicate that as the GV drops, the GRG rises. Figure 7 illustrates that the optimum GV to attain a larger GRG is 30 V. The dielectric particles around it may melt at a lower voltage (Udaya Prakash et al., 2023). As the GV rises, the GRG decreases right away.

3.6.2 Effect of T_{on} on GRG

MRR is directly proportional to the energy produced during this pulse on time. The craters from extended spark timings will be deeper and wider, giving them an irregular finish. Conversely, a lesser spark duration aids in achieving a smooth surface finish.

Deep surface craters are left on the workpiece, and a stronger explosion is produced by a more extended T_{on}'s high discharge energy. Deep craters suggest a low quality of the surface and a large MRR. Larger T_{on} values should be used to provide a superior GRG, as Figure 8 illustrates (Soni et al., 2018). For a higher GRG, 10 μs is an appropriate T_{on}. According to the findings, a higher T_{on} causes a more excellent thermal energy transfer from the wire to the specimen, which in turn causes a higher cutting velocity. The MRR increases with the discharge energy, but the SR and kerf decrease, increasing the GRG. This is because more discharge energy causes an enormous crater, which raises the GRG, and the released energy increases with the T_{on} (Dereje et al., 2023; Sahu et al., 2022).

3.6.3 Effect of pulse off time on GRG

The total duration of the rest or gap needed for the dielectric to reionize is known as the T_{off}. This duration permits the molten liquid substance to exit the spark gap. An excessively short T_{off} may make sparks uncertain, leading to increased short-circuiting. There are more discharges in a given length of time when the T_{off} is shorter. As a result, there are more discharges, which lowers surface quality but increases machining speed. Conversely, longer machining times are produced by longer T_{off}. The operation will be slowed when the advancing servomotors retract, and the T_{off} needs to be longer than the T_{on} (Juliyana and Prakash, 2022).

TABLE 3 Experimental results.

Ex. No.	A	B	C	D	E	MRR (mm³/min)	SR (µm)	GRG	Rank
	Gap voltage (V)	Pulse on time (µs)	Pulse off time (µs)	Wire feed (m/min)	Reinforcement (wt%)				
1	30	2	2	4	3	25.514	3.38	0.587	7
2	30	2	6	6	6	21.423	3.06	0.733	1
3	30	2	10	8	9	17.262	3.57	0.472	21
4	30	6	2	6	9	33.112	3.97	0.553	11
5	30	6	6	8	3	26.104	3.3	0.624	5
6	30	6	10	4	6	25.705	3.51	0.548	12
7	30	10	2	8	6	39.086	3.98	0.693	3
8	30	10	6	4	9	31.122	3.74	0.559	10
9	30	10	10	6	3	25.689	3.59	0.527	14
10	50	2	2	4	3	21.058	3.3	0.583	8
11	50	2	6	6	6	16.457	3.43	0.506	16
12	50	2	10	8	9	13.54	4.02	0.375	26
13	50	6	2	6	9	26.772	3.4	0.592	6
14	50	6	6	8	3	20.165	3.66	0.469	22
15	50	6	10	4	6	19.543	3.07	0.711	2
16	50	10	2	8	6	31.742	3.45	0.637	4
17	50	10	6	4	9	22.764	3.57	0.507	15
18	50	10	10	6	3	20.549	3.59	0.487	19
19	70	2	2	4	3	12.321	3.24	0.563	9
20	70	2	6	6	6	9.995	3.86	0.382	25
21	70	2	10	8	9	8.378	4.21	0.333	27
22	70	6	2	6	9	16.365	3.97	0.395	24
23	70	6	6	8	3	12.339	3.4	0.497	18
24	70	6	10	4	6	11.429	3.45	0.477	20
25	70	10	2	8	6	18.475	3.49	0.500	17
26	70	10	6	4	9	14.489	3.65	0.439	23
27	70	10	10	6	3	12.719	3.29	0.541	13

The experiment's results demonstrate that the GRG value decreases with increase in pulse off time. Because of the more extended non-cutting period, a greater T_{off} causes a decrease in cutting velocity. A prolonged T_{off} narrows the gap but also gives the debris particles in the gap more time to be flushed out. The ideal T_{off} is always employed to stop the aberrant process or avoid wire rupture (Çakıroğlu and Günay, 2020). The cutting rate increased during machining with a shorter T_{off} and more discharges in
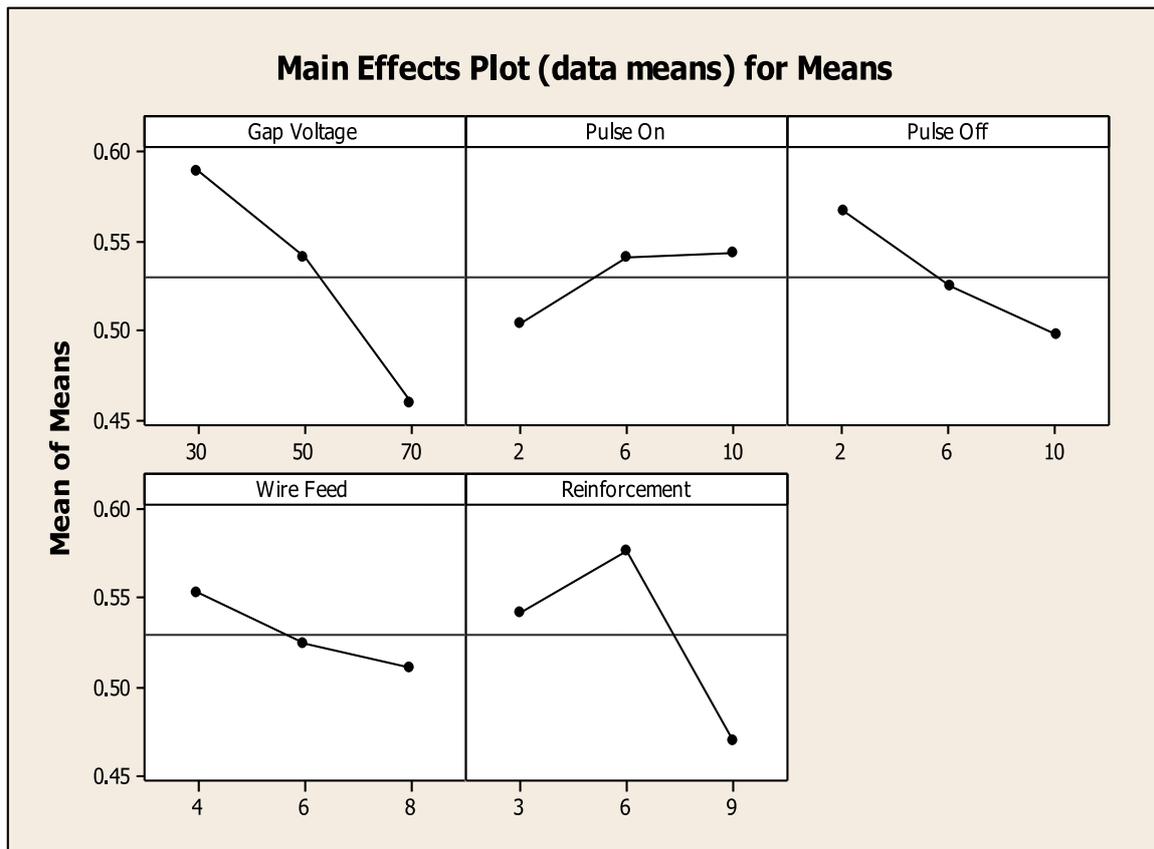
FIGURE 6
Response graphs for GRG.

TABLE 4 Response table for GRG (LM6/B$_4$C/Fly Ash).

Level	Gap voltage	Pulse on	Pulse off	Wire feed	Reinforcement
1	**0.588**	0.504	**0.567**	**0.553**	0.542
2	0.541	0.541	0.524	0.524	**0.576**
3	0.459	**0.543**	0.497	0.511	0.469
Delta	0.129	0.039	0.070	0.042	0.107
Rank	1	5	3	4	2

The bold values are the optimum levels.

a given period, leaving giant craters and surface micro-damage. Figure 9 illustrates that the ideal T_{off} to attain a greater GRG is 2 µs (Yan et al., 2021).

3.6.4 Effect of WF on GRG

A neutral input variable is the wire feed. It is essential to select the wire feed so that the wire is not damaged. As wire velocity rises, the GRG grows, as Figure 10 illustrates. The ideal wire feed setting is 4 m/min (Kumar et al., 2024) to attain the highest GRG and avoid wire failure. The outcomes of this research remained unchanged even though it was done on various materials.

3.6.5 Effect of reinforcement % on GRG

One unaffected input variable is the percentage of reinforcement. Figure 11 noted that the GRG for 6% hybrid composites is maximum. In summary, the investigation's findings were consistent with those reported in the literature. The outcomes were constant even though this study was done on various materials.

TABLE 5 ANOVA for GRG (LM6/B$_4$C/Fly Ash).

Source of variation	DOF	Sum of squares	Mean sum of squares	F$_0$	Contribution (%)
A	2	0.078	0.039	9.75	29.89%
C	2	0.023	0.012	2.88	8.81%
E	2	0.054	0.027	6.75	20.69%
AC	4	0.025	0.006	1.56	9.57%
AE	4	0.031	0.008	1.94	11.88%
Error (Pooled)	12	0.050	0.004		19.16%
Total	26	0.261			100%

FIGURE 7
Effect of GV on GRG.

FIGURE 9
Effect of Pulse off time on GRG.

FIGURE 8
Effect of pulse on time on GRG.

FIGURE 10
Effect of Wire feed on GRG.
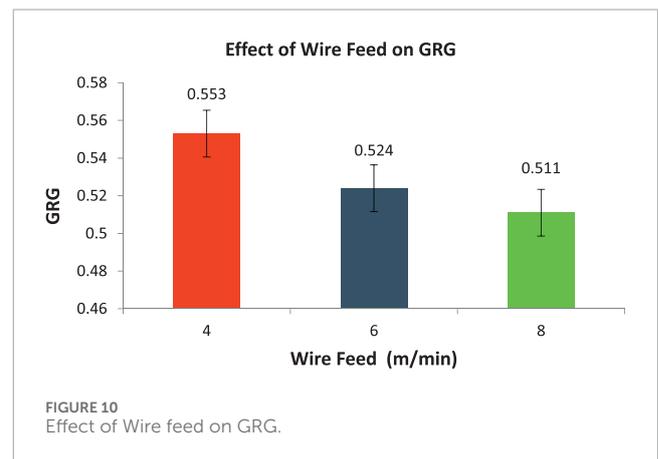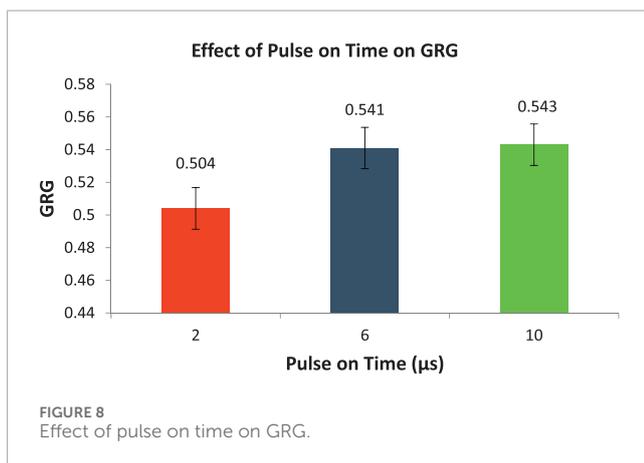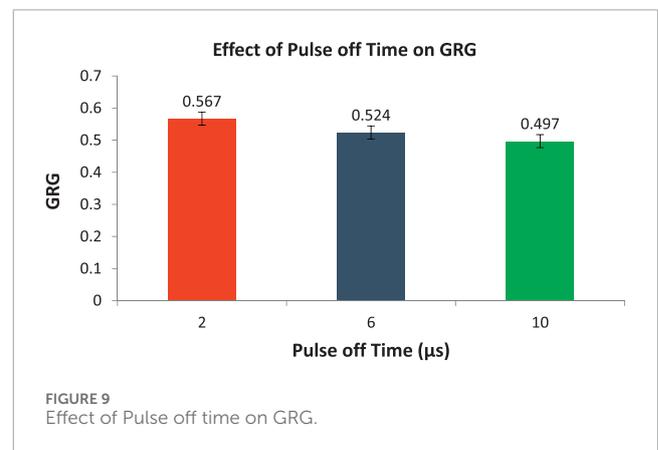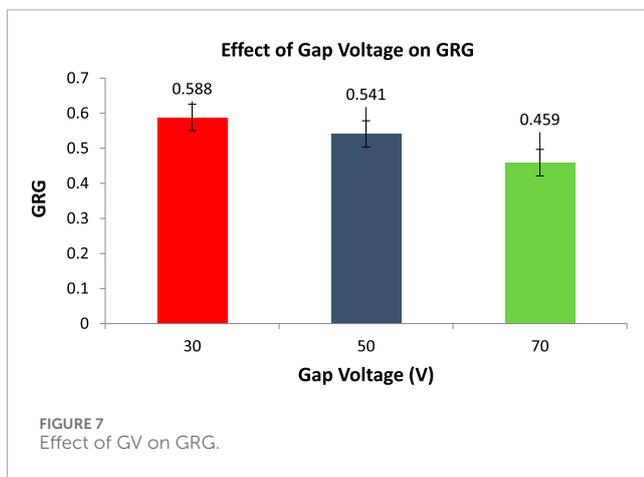
3.7 Discussion on responses

3.7.1 Material removal rate

Longer pulse on time provide more energy and produce more heat at that moment, which is useful for obtaining more MRR, but the surface finish decreases (Pramanik and Basak, 2019). Reducing T$_{off}$ increases cutting speed. The GV regulates the advance and retracts of the wire and acts as a reference voltage. The number of sparks is limited, the electric discharge is stabilized, and the cutting rate decreases when the GV rises because the space between the specimen and the wire widens (Lingadurai et al., 2012). When the GV is lowered, the average gap gets smaller, raising the number of electric sparks and machining rate and enhancing the wire breakage probability. Peak current, measured in amps, is the phrase used

FIGURE 11
Effect of reinforcement % on GRG.
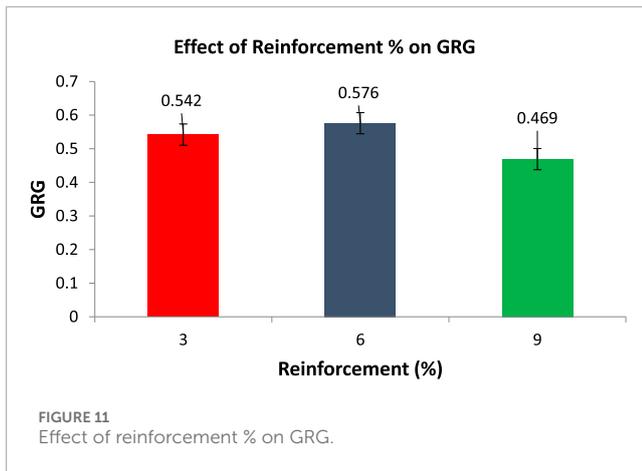
to describe the quantity of power used in discharge machining (Rashedul et al., 2021). Reducing the time between pulses will improve cutting speed. Peak current directly correlates with an increase in MRR (Nair et al., 2024).

3.7.2 Surface roughness

The amount of electric discharge is determined by the gap voltage, peak current increases with the gap voltage, leading to a higher SR. The dielectric flow rate is the frequency at which the dielectric fluid is pumped during effective machining. The wire feed rate will increase the amount of wire used and the machining cost. Wire breaks when cutting at an elevated current with a low wire speed. Within a specific range, increasing the tension of the wire significantly increases cutting speed and accuracy. The most substantial impact of discharge current on SR has been determined to be (Sivaprakasam et al., 2022; Aldrin Raj et al., 2020), with pulse duration. WEDM report states that as T_{on}, GV, and I rise, the SR increases, and the SR decreases as T_{off} rises (Saini et al., 2013).

4 Conclusion

The following conclusions can be drawn from the Optimization of WEDM Process Parameters for Machining Hybrid Composites (LM6/B$_4$C/Fly Ash) using Grey relational analysis.

1) Hybrid composites in three different weight percentages were produced using the low cost stir casting method.
2) Optical micrographs confirmed that the reinforcement was distributed uniformly throughout the matrix.
3) Gap voltage (29.89%) and Pulse off time (20.69%) are the most significant variables, affecting the GRG.
4) The optimum machining parameters for achieving higher MRR and lower SR are GV 30 V, T_{on} "10"μs, "T_{off}" 2 μs, "WF" 4 m/min, and "R" 6%.

5) The predicted value of GRG is 0.711; however the experimental GRG value is 0.733. The error is 2.2% which is acceptable, so the optimization holds good.
6) The hybrid composite produced is new and many new combinations may be produced and various optimization techniques may be used in future.

Data availability statement

The original contributions presented in the study are included in the article/supplementary material, further inquiries can be directed to the corresponding author.

Author contributions

JP: Conceptualization, Data curation, Formal Analysis, Funding acquisition, Investigation, Methodology, Project administration, Resources, Software, Supervision, Validation, Visualization, Writing–original draft, Writing–review and editing. CS: Conceptualization, Data curation, Formal Analysis, Funding acquisition, Investigation, Methodology, Project administration, Resources, Software, Supervision, Validation, Visualization, Writing–original draft, Writing–review and editing. SJ: Conceptualization, Data curation, Formal Analysis, Funding acquisition, Investigation, Methodology, Project administration, Resources, Software, Supervision, Validation, Visualization, Writing–original draft, Writing–review and editing. SS: Conceptualization, Data curation, Formal Analysis, Funding acquisition, Investigation, Methodology, Project administration, Resources, Software, Supervision, Validation, Visualization, Writing–original draft, Writing–review and editing. HÖ: Conceptualization, Data curation, Formal Analysis, Funding acquisition, Investigation, Methodology, Project administration, Resources, Software, Supervision, Validation, Visualization, Writing–original draft, Writing–review and editing. LC: Conceptualization, Data curation, Formal Analysis, Funding acquisition, Investigation, Methodology, Project administration, Resources, Software, Supervision, Validation, Visualization, Writing–original draft, Writing–review and editing.

Funding

been done in connection with project Students Grant Competition SP2024/087 "Specific Research of Sustainable Manufacturing Technologies," financed by the Ministry of Education, Youth and Sports and Faculty of Mechanical Engineering VŠB-TUO

Conflict of interest

The authors declare that the research was conducted in the absence of any commercial or financial relationships that could be construed as a potential conflict of interest.

Generative AI statement

The authors declare that no Generative AI was used in the creation of this manuscript.

Publisher's note

All claims expressed in this article are solely those of the authors and do not necessarily represent those of their affiliated organizations, or those of the publisher, the editors and the reviewers. Any product that may be evaluated in this article, or claim that may be made by its manufacturer, is not guaranteed or endorsed by the publisher.

References

Aldrin Raj, J., Balasubramanian, K., Palanisamy, D., and Emmanuel, A. G. S. (2020). Experimental investigations on WEDM process for machining high manganese steel. *Mater. Manuf. Process.* 35 (14), 1612–1621. doi:10.1080/10426914.2020.1779941

Ananth, S., Prakash, J. U., Juliyana, S. J., Rubi, C. S., and Sadhana, A. D. (2021). Effect of process parameters on WEDM of Al–Fly ash composites using Taguchi Technique. *Mater. Today Proc.* 39, 1786–1790. doi:10.1016/j.matpr.2020.07.615

Bains, P. S., Sidhu, S. S., and Payal, H. S. (2016). Fabrication and machining of metal matrix composites: a review. *Mater. Manuf. Process.* 31 (5), 553–573. doi:10.1080/10426914.2015.1025976

Çakıroğlu, R., and Günay, M. (2020). Comprehensive analysis of material removal rate, tool wear and surface roughness in electrical discharge turning of L2 tool steel. *J. Mater. Res. Technol.* 9, 7305–7317. doi:10.1016/j.jmrt.2020.04.060

Calvo, R., and Daniel, M. (2019). Wire electrical discharge machining (EDM) setup parameters influence in functional surface roughness. *Procedia Manuf.* 41, 602–609. doi:10.1016/j.promfg.2019.09.048

Dereje, T., Palani, S., Desta, M., and Čep, R. (2023). Experimental investigation into the influence of the process parameters of wire electric discharge machining using nimonic-263 superalloy. *Materials* 16 (15), 5440. doi:10.3390/ma16155440

Durairaj, M., Sudharsun, D., and Swamynathan, N. (2013). Analysis of process parameters in wire EDM with stainless steel using single objective Taguchi method and multi objective grey relational grade. *Procedia Eng.* 64, 868–877. doi:10.1016/j.proeng.2013.09.163

Fanani, E. W., Surojo, E., Prabowo, A. R., and Akbar, H. I. (2021). Recent progress in hybrid aluminum composite: manufacturing and application. *Metals* 11 (12), 1919. doi:10.3390/met11121919

Goswami, A., and Kumar, J. (2014). Optimization in wire-cut EDM of Nimonic-80A using Taguchi's approach and utility concept. *Eng. Sci. Technol. Int. J.* 17 (4), 236–246. doi:10.1016/j.jestch.2014.07.001

Goyal, A., Pandey, A., Sharma, P., and Sharma, S. K. (2017). Study on Ni-based super alloy using cryogenic treated electrode by Taguchi methodology. *Mater. Today Proc.* 4, 2068–2076. doi:10.1016/j.matpr.2017.02.052

Goyal, K. K., Sharma, N., Dev Gupta, R., Singh, G., Rani, D., Banga, H. K., et al. (2022). A soft computing-based analysis of cutting rate and recast layer thickness for AZ31 alloy on WEDM using RSM-MOPSO. *Materials* 15 (2), 635. doi:10.3390/ma15020635

Jayaseelan, V., Kalaichelvan, K., Ramasamy, N., and Seeman, M. (2023). Influence of SiCp volume percentage on AA6063/SiCp MMC extrusion process: an experimental, theoretical and simulation analysis. *Int. J. Lightweight Mater. Manuf.* 6 (3), 357–366. doi:10.1016/j.ijlmm.2023.03.001

JebaroseJuliyana, S., Udaya Prakash, J., Čep, R., and Karthik, K. (2023a). Multi-objective optimization of machining parameters for drilling LM5/ZrO2 composites using grey relational analysis. *Materials* 16 (10), 3615. doi:10.3390/ma16103615

JebaroseJuliyana, S., Udaya Prakash, J., Rubi, C. S., Salunkhe, S., Gawade, S. R., Abouel Nasr, E. S., et al. (2023b). Optimization of wire EDM process parameters for machining hybrid composites using grey relational analysis. *Crystals* 13 (11), 1549. doi:10.3390/cryst13111549

Juliyana, S. J., and Prakash, J. U. (2022). Optimization of machining parameters for wire EDM of AMCs (LM5/ZrO2) using Taguchi technique. *INCAS Bull.* 14 (1), 57–68. doi:10.13111/2066-8201.2022.14.1.5

Juliyana, S. J., Prakash, J. U., Sadhana, A. D., and Rubi, C. S. (2022b). Multi-objective optimization of process parameters of wire EDM for machining of AMCs (LM5/ZrO2) using grey relational analysis. *Mater. Today Proc.* 52, 1494–1498. doi:10.1016/j.matpr.2021.11.213

Juliyana, S. J., Prakash, J. U., and Salunkhe, S. (2022c). Optimisation of wire EDM process parameters using Taguchi technique for machining of hybrid composites. *Int. J. Mater. Eng. Innovation* 13 (3), 257–271. doi:10.1504/ijmatei.2022.125110

Juliyana, S. J., Prakash, J. U., Salunkhe, S., Hussein, H. M., and Gawade, S. R. (2022a). Mechanical characterization and microstructural analysis of hybrid composites (LM5/ZrO2/Gr). *Crystals* 12 (9), 1207. doi:10.3390/cryst12091207

Karthik, S., Prakash, K. S., Gopal, P. M., and Jothi, S. (2019). Influence of materials and machining parameters on WEDM of Al/AlCoCrFeNiMo 0.5 MMC. *Mater. Manuf. Process.* 34 (7), 759–768. doi:10.1080/10426914.2019.1594250

Kumar, A., Grover, N., Manna, A., Kumar, R., Chohan, J. S., Singh, S., et al. (2022). Multi-objective optimization of WEDM of aluminum hybrid composites using AHP and genetic algorithm. *Arabian J. Sci. Eng.* 47 (7), 8031–8043. doi:10.1007/s13369-021-05865-4

Kumar, A., Kumar, V., and Kumar, J. (2013). Investigation of machining parameters and surface integrity in wire electric discharge machining of pure titanium. *Proc. IMechE Part B J. EngManufact* 227 (7), 972–992. doi:10.1177/0954405413479791

Kumar, A., Soota, T., and Kumar, J. (2018). Optimisation of wire-cut EDM process parameter by Grey-based response surface methodology. *J. Industrial Eng. Int.* 14 (4), 821–829. doi:10.1007/s40092-018-0264-8

Kumar, A., Upadhyay, C., Kumar, N., Ram Prasad, A. V., and Nagaraju, D. S. (2024). Soft computing based parametric optimization of cutting rate, surface roughness, and kerf width in wire electric discharge machining of high strength Ti-3Al-2.5 V. *Exp. Tech.* 48 (3), 537–558. doi:10.1007/s40799-023-00681-x

Laghari, R. A., Jamil, M., Laghari, A. A., Khan, A. M., Akhtar, S. S., and Mekid, S. (2023). A critical review on tool wear mechanism and surface integrity aspects of SiCp/Al MMCs during turning: prospects and challenges. *Int. J. Adv. Manuf. Technol.* 126 (7), 2825–2862. doi:10.1007/s00170-023-11178-7

Lee, H. T., and Tai, T. Y. (2003). Relationship between EDM parameters and surface crack formation. *J. Mater Process Technol.* 142, 676–683. doi:10.1016/s0924-0136(03)00688-5

Lingadurai, K., Nagasivamuni, B., Muthu Kamatchi, M., and Palavesam, J. (2012). Selection of wire electrical discharge Machining Process parameters on stainless steel AISI grade-304 using Design of experiments approach. *J. Institution Eng. India Ser. C* 93 (2), 163–170. doi:10.1007/s40032-012-0020-6

Lodhi, B. K., and Agarwal, S. (2014). Optimization of machining parameters in WEDM of AISI D3 steel using taguchi technique. *Procedia CIRP* 14, 194–199. doi:10.1016/j.procir.2014.03.080

Magabe, R., Sharma, N., Gupta, K., and Paulo Davim, J. (2019). Modeling and optimization of Wire-EDM parameters for machining of Ni55.8Ti shape memory alloy using hybrid approach of Taguchi and NSGA-II. *Int. J. Adv. Manuf. Technol.* 102 (5–8), 1703–1717. doi:10.1007/s00170-019-03287-z

Manjaiah, M., Laubscher, R. F., Kumar, A., and Basavarajappa, S. (2016). Parametric optimization of MRR and surface roughness in wire electro discharge machining (WEDM) of D2 steel using Taguchi-based utility approach. *Int. J. Mech. Mater. Eng.* 11 (1), 7. doi:10.1186/s40712-016-0060-4

Marelli, D., Singh, S. K., Nagari, S., and Subbiah, R. (2019). Optimisation of machining parameters of wire-cut EDM on super alloy materials-A review. *Mater. Today Proc.* 26, 1021–1027. doi:10.1016/j.matpr.2020.01.306

Nair, H., Pramanik, A., Basak, A. K., Prakash, C., Debnath, S., Shankar, S., et al. (2024). Experimental investigation on material removal rate, kerf width, surface roughness and the dimensional accuracy the accuracy of hole in Inconel 718 using wire electric discharge. *Proc. Institution Mech. Eng. Part E J. Process Mech. Eng.* 238 (3), 1017–1030. doi:10.1177/09544089221096025

Nourbakhsh, F., Rajurkar, K. P., Malshe, A. P., and Cao, J. (2013). Wire electro-discharge machining of titanium alloy. *Procedia CIRP* 5, 13–18. doi:10.1016/j.procir.2013.01.003

Omole, S., Lunt, A., Kirk, S., and Shokrani, A. (2022). Advanced processing and machining of tungsten and its alloys. *J. Manuf. Mater. Process.* 6 (1), 15. doi:10.3390/jmmp6010015

Parikh, V. K., Badheka, V. J., Badgujar, A. D., and Ghetiya, N. D. (2021). Fabrication and processing of aluminum alloy metal matrix composites. *Mater. Manuf. Process.* 36, 1604–1617. doi:10.1080/10426914.2021.1914848

Paulson, D. M., Saif, M., and Zishan, M. (2023). Optimization of wire-EDM process of titanium alloy-Grade 5 using Taguchi's method and grey relational analysis. *Mater. Today Proc.* 72, 144–153. doi:10.1016/j.matpr.2022.06.376

Peter, J. M., Udaya Prakash, J., and Moorthy, T. V. (2014). Optimization of WEDM process parameters of hybrid composites (A413/B4C/Fly Ash) using grey relational analysis. *Appl. Mech. Mater.* 592, 658–662. doi:10.4028/www.scientific.net/amm.592-594.658

Prakash, J. U., JebaroseJuliyana, S., Salunkhe, S., Gawade, S. R., Nasr, E. S., and Kamrani, A. K. (2023a). Mechanical characterization and microstructural analysis of stir-cast aluminum matrix composites (LM5/ZrO2). *Crystals* 13 (8), 1220. doi:10.3390/cryst13081220

Prakash, J. U., Juliyana, S. J., Pallavi, P., and Moorthy, T. V. (2018). Optimization of wire EDM process parameters for machining hybrid composites (356/B4C/Fly ash) using Taguchi technique. *Mater. Today Proc.* 5 (2), 7275–7283. doi:10.1016/j.matpr.2017.11.395

Prakash, J. U., Sivaprakasam, P., Garip, I., Juliyana, S. J., Elias, G., Kalusuraman, G., et al. (2021). Wire electrical discharge machining (WEDM) of hybrid composites (Al-Si12/B4C/Fly ash). *J. Nanomater.* 2021, 1–10. doi:10.1155/2021/2503673

Prakash, J. U., Sivaprakasam, P., Juliyana, S. J., Ananth, S., Rubi, C. S., and Sadhana, A. D. (2023b). Multi-objective optimization using grey relational analysis for wire EDM of aluminium matrix composites. *Mater. Today Proc.* 72, 2395–2401. doi:10.1016/j.matpr.2022.09.415

Pramanik, A., and Basak, A. K. (2019). Effect of wire electric discharge machining (EDM) parameters on fatigue life of Ti-6Al-4V alloy. *Int. J. Fatigue* 128, 105186. doi:10.1016/j.ijfatigue.2019.105186

Pramanik, A., Islam, M. N., Basak, A. K., Dong, Y., Littlefair, G., and Prakash, C. (2019). Optimizing dimensional accuracy of titanium alloy features produced by wire electrical discharge machining. *Mater. Manuf. Process.* 34 (10), 1083–1090. doi:10.1080/10426914.2019.1628259

Qudeiri, J. E., Zaiout, A., Mourad, A. H., Abidi, M. H., and Elkaseer, A. (2020). Principles and characteristics of different EDM processes in machining tool and die steels. *Appl. Sci.* 10 (6), 2082. doi:10.3390/app10062082

Ramanan, G., and Edwin Raja Dhas, J. (2017). Multi objective optimization of machining parameters for AA7075 metal matrix composite using grey - fuzzy technique. *Int. J. Appl. Eng. Res.* 12 (8), 1729–1735.

Rashedul, I. M., Zhang, Y., Zhou, K., Wang, G., Xi, T., and Ji, L. (2021). Influence of different tool electrode materials on electrochemical discharge machining performances. *Micromachines* 12 (9), 1077. doi:10.3390/mi12091077

Rubi, C. S., and Prakash, J. U. (2020). Drilling of hybrid aluminum matrix composites using Grey-Taguchi Method. *INCAS Bull.* 12 (1), 167–174. doi:10.13111/2066-8201.2020.12.1.16

Rubi, C. S., Prakash, J. U., Rajkumar, C., Mohan, A., and Muthukumarasamy, S. (2022). Optimization of process variables in drilling of LM6/fly ash composites using Grey-Taguchi method. *Mater. Today Proc.* 62, 5894–5898. doi:10.1016/j.matpr.2022.04.627

Sadhana, A. D., Prakash, J. U., Sivaprakasam, P., and Ananth, S. (2020). Wear behaviour of aluminium matrix composites (LM25/Fly ash)–A Taguchi approach. *Mater. Today Proc.* 33, 3093–3096. doi:10.1016/j.matpr.2020.03.684

Sahu, N. K., Singh, M. K., GetrudeMutono-Mwanza, B., and Sahu, A. K. (2022). Investigation of machinability characteristics of EDMed inconel 825 alloy under multidimensional parametric modeling by using holistic grey-PCA statistical models. *Adv. Mater. Sci. Eng.* 2022 (1), 1–29. doi:10.1155/2022/3147586

Saini, V. K., Khan, Z. A., and Siddiquee, A. N. (2013). Optimization of wire electric discharge machining of composite material (Al6061/SiCp) using Taguchi method. *Int. J. Mech. Prod. Eng.* 2 (1), 61–64.

Sarala Rubi, C., Prakash, J. U., Juliyana, S. J., Čep, R., Salunkhe, S., Kouril, K., et al. (2024). Comprehensive review on wire electrical discharge machining: a non-traditional material removal process. *Front. Mech. Eng.* 10. doi:10.3389/fmech.2024.1322605

Silambarasan, S., and Prabhakaran, G. (2019). Optimization of process parameters of wire EDM using genetic. *Int. J. Mech. Prod. Eng. Res. Dev.* 8, 426–430.

Singh, B., and Misra, J. P. (2018). Empirical modeling of average cutting speed during WEDM of gas turbine alloy. *MATEC Web Conf.* 221, 01002. doi:10.1051/matecconf/201822101002

Singh, V., and Pradhan, S. K. (2014). Optimization of WEDM parameters using taguchi technique and response surface methodology in machining of AISI D2 steel. *Procedia Eng.* 97, 1597–1608. doi:10.1016/j.proeng.2014.12.310

Sivaprakasam, P., Udaya Prakash, J., and Hariharan, P. (2022). Enhancement of material removal rate in magnetic field-assisted micro electric discharge machining of Aluminium Matrix Composites. *Int. J. Ambient Energy* 43 (1), 584–589. doi:10.1080/01430750.2019.1653979

Somashekhar, K. P., Mathew, J., and Ramachandran, N. (2012). A feasibility approach by simulated annealing on optimization of micro-wire electric discharge machining parameters. *Int. J. Adv. Manuf. Technol.* 61, 1209–1213. doi:10.1007/s00170-012-4096-1

Soni, H., Narendranath, S., and Ramesh, M. R. (2018). Experimental investigation on effects of wire electro discharge machining of Ti50Ni45Co5 shape memory alloys. *Silicon* 10, 2483–2490. doi:10.1007/s12633-018-9780-9

Srinivasa Rao, P., Ramji, K., and Satyanarayana, B. (2016). Effect of wire EDM conditions on generation of residual stresses in machining of aluminum 2014 T6 alloy. *Alexandria Eng. J.* 55 (2), 1077–1084. doi:10.1016/j.aej.2016.03.014

Thangaraj, M., Annamalai, R., Moiduddin, K., Alkindi, M., Ramalingam, S., and Alghamdi, O. (2020). Enhancing the surface quality of micro titanium alloy specimen in WEDM process by adopting TGRA-Based optimization. *Materials* 13 (6), 1440. doi:10.3390/ma13061440

Udaya Prakash, J., JebaroseJuliyana, S., Saleem, M., and Moorthy, T. V. (2021). Optimisation of dry sliding wear parameters of aluminium matrix composites (356/B4C) using Taguchi technique. *Int. J. Ambient Energy* 42 (2), 140–142. doi:10.1080/01430750.2018.1525590

Udaya Prakash, J., Rajkumar, C., Jayavelu, S., and Sivaprakasam, P. (2023). Effect of wire electrical discharge machining parameters on various tool steels using grey relational analysis. *Int. J. Veh. Struct. and Syst.* 15 (2), 203–206. doi:10.4273/ijvss.15.2.11

Vishwakarma, M., Parashar, V., and Khare, V. K. (2012). Advancement in Electric Discharge Machining on metal matrix composite materials in recent: a Review. *Int. J. Sci. Res. Publ.* 2 (3), 1–8.

Yan, H., Kabongo, B. D., Zhou, H., Wu, C., and Chen, Z. (2021). Analysis and optimization of the machining characteristics of high-volume content SiCp/Al composite in wire electrical discharge machining. *Crystals* 11, 1342. doi:10.3390/cryst11111342